

# Advanced Research Center for Beam Science – Electron Microscopy and Crystal Chemistry –

<http://eels.kuicr.kyoto-u.ac.jp/Root/English>



Prof  
KURATA, Hiroki  
(D Sc)



Assist Prof  
NEMOTO, Takashi  
(D Sc)



Program-Specific Res  
OGAWA, Tetsuya  
(D Sc)



Program-Specific Res  
KIYOMURA, Tsutomu



Res\*  
MORIGUCHI, Sakumi  
(D Sc)

\* Re-employed Staff

## Students

SHINODA, Yasuhiro (D3)  
SAITO, Hikaru (D2)  
ASO, Ryotaro (D2)  
FUJIYOSHI, Yoshifumi (D1)

OGIMOTO, Mao (M2)  
YAMAGUCHI, Atsushi (M1)  
YAMAGUCHI, Hitomi (M1)

## Visitor

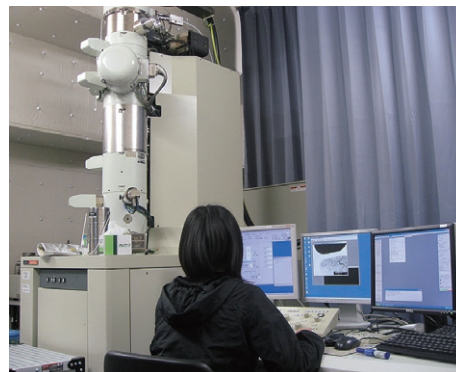
Dr LO, Shen-Chuan Industrial Technology Research Institute, Taiwan, 28 May–1 June, 15–19 October

## Scope of Research

Crystallographic and electronic structures of materials and their transformations are studied through direct imaging of atoms or molecules by high-resolution electron spectromicroscopy which realizes energy-filtered imaging and electron energy-loss spectroscopy as well as high resolution imaging. By combining this with scanning probe microscopy, the following subjects are urging: direct structure analysis, electron crystallographic analysis, epitaxial growth of molecules, structure formation in solutions, and fabrication of low-dimensional functional assemblies.

### KEYWORDS

TEM EELS  
STEM SPM  
Cryo-TEM



## Selected Publications

Kobayashi, T.; Ogawa, T.; Moriguchi, S.; Suga, T.; Yoshida, K.; Kurata, H.; Isoda, S., Inhomogeneous Substitution of Polyhalogenated Copper-phthalocyanine Studied by High-resolution Imaging and Electron Crystallography, *J. Electron Microsc.*, **52**, 85-90 (2003).  
Minari, T.; Nemoto, T.; Isoda, S., Temperature and Electric-field Dependence of the Mobility of a Single-grain Pentacene Field-effect Transistor, *J. Appl. Phys.*, **99**, 034506 (2006).  
Kiyomura, T.; Nemoto, T.; Ogawa, T.; Minari, T.; Yoshida, K.; Kurata, H.; Isoda, S., Thin-Film Phase of Pentacene Film Formed on KCl by Vacuum Deposition, *Jpn. J. Appl. Phys.*, **45**, 401-404 (2006).  
Haruta, M.; Kurata, H.; Komatsu, H.; Shimakawa, Y.; Isoda, S., Site-resolved Oxygen K-edge ELNES of Layered Double Perovskite  $\text{La}_2\text{CuSnO}_6$ , *Physical Review B*, **80**, 165123 (2009).  
Haruta, M.; Kurata, H., Direct Observation of Crystal Defects in an Organic Molecular Crystals of Copper Hexachlorophthalocyanine by STEM-EELS, *Sci. Rep.*, **2**, [252-1]-[252-4] (2012).

## Direct Observation of Crystal Defects in an Organic Molecular Crystals of Copper Hexachlorophthalocyanine by STEM-EELS

The structural analysis of crystal defects in organic thin films provides fundamental insights into their electronic properties for applications such as field effect transistors. Observation of crystal defects in organic thin films has previously been performed at rather low resolution by conventional transmission electron microscopy based on phase-contrast imaging. Herein, we apply for the first time annular dark-field imaging to the direct observation of grain boundaries in copper hexachlorophthalocyanine thin films at the atomic resolution level by using an aberration-corrected scanning transmission electron microscope combined with electron energy-loss spectroscopy. By using a low-dose technique and an optimized detection angle, we were able to visualize the contrast of light element (C and N) together with the heavier elements (Cl and Cu) within the molecular column. We were also able to identify unexpected molecular orientations in the grain boundaries along the  $\{110\}$  crystallographic planes giving rise to stacking faults.

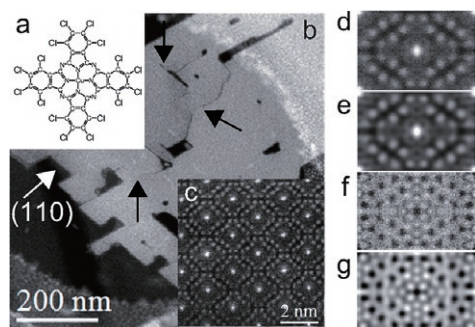


**Figure 1.** (a) Molecular structure of  $\text{Cl}_{16}\text{CuPc}$ . (b) Low-magnification image of  $\text{Cl}_{16}\text{CuPc}$  molecular crystal projected along the  $c$ -axis. (c) High resolution LAADF-STEM raw image from a single crystal region. (d) Translationally averaged experimental and (e) noise-filtered LAADF-STEM images of one molecular column. (f) Translationally averaged experimental and (g) noise-filtered ABF-STEM images of one molecular column.

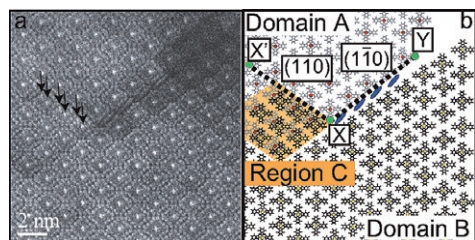


**Figure 2.** (a) LAADF-STEM image of complex defect region. The stacking fault was observed along the  $(110)$  plane and  $\text{Cl}_{16}\text{CuPc}$  molecules with irregular orientation were identified in the grain boundary along the  $(\bar{1}\bar{1}0)$  plane as a line contrast. (b) Schematic diagram of molecular columns corresponding to (a). The two domains, A and B, can be seen as gray and black molecules, and molecules along the XY grain boundary are shown as blue ellipses.

## Photoassisted Scanning Tunneling Microscopy Investigation on the ZnO(0001)-Zn Surface Treated by Alkaline Solution

In this study, the surface geometric structures of epitaxial (0001) ZnO films treated by NaOH solution are investigated using photoassisted scanning tunneling microscopy (STM). By illuminating ultraviolet (UV) light on the epitaxial (0001) ZnO film, the tunneling current can be significantly enhanced to construct the well-defined STM images. Polarity identification of the epitaxial (0001) ZnO film by convergent-beam electron diffraction indicates that the epitaxial (0001) ZnO film exhibits the Zn-polar surface. Two types of topographic features, i.e., hexagonal pyramid and flat plane, are observed in the AFM images of the as-grown epitaxial (0001) ZnO film. UV-assisted STM images reveal the anisotropic etching behaviors of the epitaxial (0001) ZnO films in NaOH solution. The faceted and symmetrically layered hexagonal-pyramid feature gets asymmetrical and rounded with increasing etching time. On the other hand, few small hexagonal pits on the as-grown flat ZnO(0001)-Zn surface are developed to asymmetrically hexagonal cavities with flat terraces and steps after NaOH treatments. In addition, triangular reconstruction of the NaOH-treated ZnO(0001)-Zn surface and evidently layerstacking feature on a faceted ZnO surface with a step height resolved in the atomic scale are also demonstrated in ambience using the photoassisted STM.

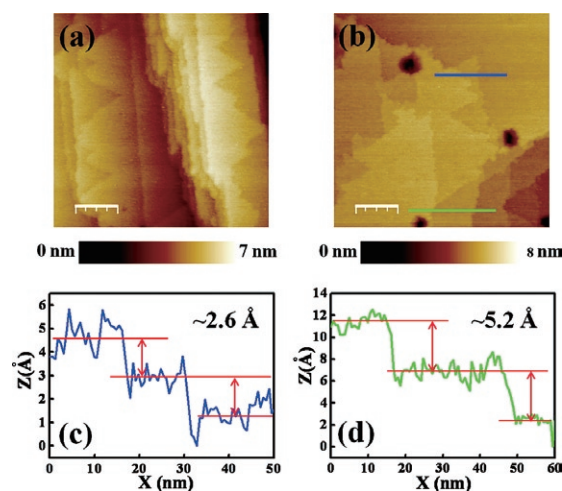


**Figure 3.** High-magnification UV-assisted STM images of ZnO films after NaOH treatments for (a) 20 s (scale bar = 30 nm) and (b) 50 s (scale bar = 32 nm). (c,d) Cross-sectional line profiles of the regions in (b) denoted by blue and green lines, respectively.